

## Dark sector freeze-out due to a non-Boltzmann suppression

---

Anirban Biswas,<sup>a</sup> Sougata Ganguly<sup>b,1,\*</sup> and Sourov Roy<sup>b</sup>

<sup>a</sup>Department of Physics, Sogang University, Seoul 121-742, South Korea

<sup>b</sup>School of Physical Sciences, Indian Association for the Cultivation of Science

2A & 2B Raja S.C.Mullick Road, Jadavpur, Kolkata-700032, India

E-mail: [anirban.biswas.sinp@gmail.com](mailto:anirban.biswas.sinp@gmail.com), [ganguly.sougata@gmail.com](mailto:ganguly.sougata@gmail.com),

[tps@iacs.res.in](mailto:tps@iacs.res.in)

The well-known Boltzmann suppression is the key ingredient to create chemical imbalance for thermal dark matter. In a degenerate/quasi-degenerate dark sector chemical imbalance can also be generated from a different mechanism which is analogous to the radioactive decay law, known as co-decaying dark matter. In this work, we have studied the dynamics of a multicomponent thermally decoupled degenerate dark sector in a hidden  $U(1)_X$  extension of the Standard Model. We compute the relic density and the temperature ( $T'$ ) evolution of the hidden sector by considering all possible  $2 \rightarrow 2$  and  $3 \rightarrow 2$  processes. We find that the production of energetic particles from  $3 \rightarrow 2$  processes increase the temperature of the dark sector whereas the rate of growth of temperature is decelerated due to the presence of  $2 \rightarrow 2$  processes and expansion of the Universe. We also study the prospect of detecting neutrino and  $\gamma$ -ray signals from DM annihilation via one step cascade processes. We find that in the present scenario, all the existing indirect detection constraints arising from measured fluxes of atmospheric neutrinos by Super-Kamiokande and diffuse  $\gamma$ -rays by EGRET, Fermi-LAT, and INTEGRAL can easily be evaded for the degenerate dark sector. However for the quasi degenerate scenario the constraints are significant.

*41st International Conference on High Energy physics - ICHEP2022*

*6-13 July, 2022*

*Bologna, Italy*

---

<sup>1</sup>I would like to thank University Grants Commission (UGC), Science and Engineering Research Board (SERB), and Indian Association for the Cultivation of Science for financial support.

\*Speaker

## 1. Introduction

The notion of secluded dark sector [1–4] was introduced to explain the null results of the direct searches. In the secluded dark sector (DS) framework, DS contains a dark matter (DM) candidate and a mediator particle which acts as a portal between the dark and visible sectors. The key assumption in this scenario is that the portal coupling should be tiny enough to evade all the observational constraints but sufficient to establish kinetic equilibrium between visible and dark sectors.

In this talk, based on [5], we have discussed the dynamics of a secluded thermally decoupled multicomponent dark sector where the dark sector particles are degenerate/quasi-degenerate. Here we have considered an anomaly free  $U(1)_X$  extension of the standard model (SM). The dark sector contains two Majorana fermion DM  $\chi_1$  and  $\chi_2$ , the gauge boson corresponding to the  $U(1)_X$  gauge symmetry and a real scalar  $h_d$  which is originated after the  $U(1)_X$  breaking scalar  $\Phi$  acquires a non-zero vacuum expectation value. In this set-up, the dark and visible sectors are connected through the kinetic mixing parameter ( $\epsilon$ ) between  $U(1)_X$  and SM  $U(1)_Y$  groups and the scalar mixing angle ( $\alpha$ ) between  $h_d$  and SM Higgs boson ( $h$ ). As we do not have any a priori knowledge about the couplings within the dark sector, we have assumed that all the dark sector couplings are of same order. The choice of universal couplings within the dark sector leads to a degenerate/quasi-degenerate dark sector. Due to the degeneracy of the dark sector particles, the DM freezes-out when the mediator particles decay out-of-equilibrium to the SM particles. This mechanism is known as ‘‘co-decaying dark matter’’ [6].

Here, we have assumed that both the sectors are thermally decoupled by choosing the portal couplings accordingly. Considering all possible  $2 \rightarrow 2$  and  $3 \rightarrow 2$  processes, we have studied the DM relic density as well as dark sector temperature ( $T'$ ) evolution. It was observed that due to the presence of  $3 \rightarrow 2$  processes, the dark sector enters into the cannibal phase. In addition to that, we have investigated the prospect of detecting  $\nu$  and  $\gamma$  ray signal from DM annihilation via one-step cascade processes along with the other experimental constraints from direct detection, thermalisation of visible and dark sector, DM self interaction, SN1987A cooling, big bang nucleosynthesis (BBN), beam-dump experiments, electroweak precision observables (EWPO).

## 2. The Model

We have considered a  $SU(3)_C \otimes SU(2)_L \otimes U(1)_Y \otimes U(1)_X$  gauge invariant theory where all the SM fields are singlet under  $U(1)_X$  gauge symmetry. We extend the fermionic sector of the SM by adding two SM gauge singlet left chiral Weyl fermions  $\xi_{1L}$  and  $\xi_{2L}$  with  $U(1)_X$  charge 1 and  $-1$  respectively. We also extend the scalar sector of SM by adding a complex scalar  $\eta$  with  $U(1)_X$  charge  $-2$ . The Lagrangian of the model is given by

$$\begin{aligned} \mathcal{L} = & \mathcal{L}_{\text{SM}} - \frac{1}{4} X_{\mu\nu} X^{\mu\nu} - \frac{\epsilon}{2} B_{\mu\nu} X^{\mu\nu} + i \overline{\xi_{1L}} \not{D} \xi_{1L} + i \overline{\xi_{2L}} \not{D} \xi_{2L} + (D_\mu \eta)^\dagger (D^\mu \eta) \\ & - \left( \frac{y_1}{2} \overline{\xi_{1L}^c} \xi_{1L} \eta + \frac{y_2}{2} \overline{\xi_{2L}^c} \xi_{2L} \eta^\dagger \right) - V(\Phi, \eta) \end{aligned} \quad (1)$$

where,

$$V(\Phi, \eta) = -\mu_X^2 (\eta^\dagger \eta) + \lambda_X (\eta^\dagger \eta)^2 + \lambda' (\eta^\dagger \eta) (\Phi^\dagger \Phi) \quad (2)$$

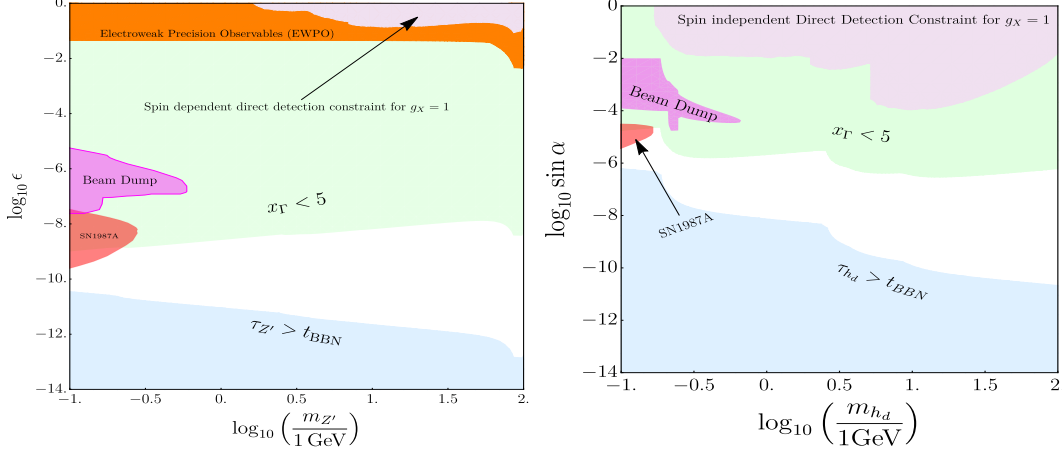


**Figure 1:** *Left panel:* Allowed parameter space in the  $m_{Z'} - \epsilon$  plane. The light blue shaded region is disallowed from the BBN and the light green region is disallowed from the requirement of a kinetically decoupled dark sector. The Magenta and red shaded regions are disallowed from Beam dump experiments and SN 1987A cooling respectively. The Constraints from EWPO and direct detection cross section are shown by the orange and the purple coloured regions respectively. *Right panel:* Allowed parameter space in  $m_{h_d} - \sin \alpha$  plane. Colour code is same as the left panel. Figures are taken from [5].

Here  $\Phi$  is the SM Higgs doublet,  $\xi_{iL}^c = C \overline{\xi_{iL}^T}$ , ( $i = 1, 2$ ) and  $C$  is the charge conjugation operator. The field strength tensor of the extra  $U(1)_X$  gauge symmetry is  $X_{\mu\nu} = \partial_\mu X_\nu - \partial_\nu X_\mu$  while the corresponding tensor of  $U(1)_Y$  gauge symmetry of the SM is  $B_{\mu\nu}$ . Note that there could exist a term  $m_{12} \overline{\xi_{1L}^c} \xi_{2L}$  which triggers mixing between  $\xi_{1L}$  and  $\xi_{2L}$ . However, we have avoided such term by assuming one of the two chiral fermions as  $\mathbb{Z}_2$  odd. After diagonalising the mass matrices, one can write Eq. 1 in terms of  $\chi_1, \chi_2, Z'$ , and  $h_d$  where  $\chi_i$  ( $i = 1, 2$ ) is a Majorana fermion DM. The dark vector boson  $Z'$  and dark sector Higgs  $h_d$  couple with the SM fields through the kinetic mixing parameter ( $\epsilon$ ) and the mixing angle between  $h_d$  and SM Higgs boson ( $\alpha$ ) respectively.

### 3. Constraints on the portals

There exist various constraints on the portal couplings from cosmological, astrophysical, and laboratory searches. In Fig. 1 we show the constraints on portal couplings ( $\epsilon, \alpha$ ) and masses of the mediator particles ( $m_{Z'}, m_{h_d}$ ) from BBN (light blue), direct detection experiments (purple), thermalisation condition (light green), SN1987A cooling (light red), beam dump experiments (magenta). In addition to that the kinetic mixing portal can also be constrained from the electroweak precision observables (EWPO) and the EWPO constraint is shown by the orange colored region in the left panel of Fig. 1.

### 4. Numerical Results

We have numerically solved four coupled Boltzmann equations for  $Y_\chi = Y_{\chi_1} + Y_{\chi_2}, Y_{Z'}, Y_{h_d}$ , and  $T'$  to find the evolution of comoving number densities of dark sector particles and temperature evolution of the dark sector using  $x = 0.1, \xi = 0.1$  (i.e.  $x' = 1$ ) and  $Y_i = Y_i^{\text{eq}}$  as initial conditions.

In Fig. 2, we choose  $m_\chi = m_{Z'} = m_{h_d} = m = 100$  MeV,  $g_X = 0.106$ ,  $\epsilon = 10^{-10}$ , and  $\alpha = 10^{-6}$  rad and the choice of the parameters is consistent with Fig. 1. In the left panel of Fig. 2, we show the evolution of  $Y_\chi$  (red solid line),  $Y_{Z'}$  (green solid line),  $Y_{h_d}$  (red solid line). The black dotted line denotes the evolution of equilibrium comoving number density of  $\chi$  ( $Y_\chi^{\text{eq}}$ ). Initially,  $Y_\chi$  follows  $Y_\chi^{\text{eq}}$  and it deviates from  $Y_\chi^{\text{eq}}$  when the mediator particles starts to decay out-of-equilibrium into SM particles. The out-of-equilibrium decay of mediator particles create chemical imbalance in the  $2 \rightarrow 2$  interactions between  $\chi_i$  and other species ( $Z'$ ,  $h_d$ ), leading to the freeze-out of DM. Since the mediator particles are long-lived due to their feeble couplings with SM particles, DM freezes-out at much later time in comparison to the weakly interacting massive particles (WIMP) scenario. In

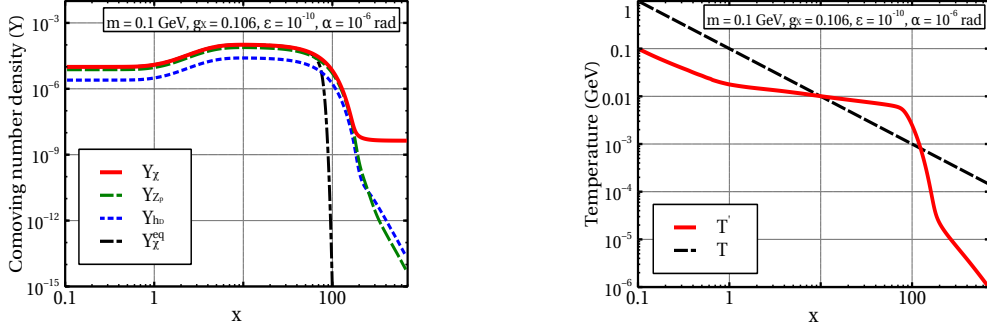


**Figure 2:** *Left panel:* Variation of comoving number densities of  $\chi_1 + \chi_2$ ,  $Z'$  and  $h_d$  with  $x = m/T$  for  $m = 100$  MeV,  $\epsilon = 10^{-10}$ ,  $g_X = 0.106$ , and  $\alpha = 10^{-6}$  rad. *Right panel:* Evolution of dark sector temperature  $T'$  with  $x$  (solid red line) for same choices of parameters, considered in the left panel. Evolution of the SM temperature is shown by the black dashed line. The choices of the parameters are motivated by the relic density constraint. Both the figures are taken from [5].

the right panel of Fig. 2, we show the evolution of  $T'$  (solid red line) as a function of  $x$  for the same choices of parameters, considered in the left panel. The black dashed line denote the evolution of SM bath temperature  $T$ . One can see from this figure,  $T'$  is almost constant between  $1 \lesssim x \lesssim 100$ . This is known as “cannibal phase” where  $3 \rightarrow 2$  processes within the dark sector are active and these processes heat up the dark sector. Finally for large  $x$  when all the processes in the dark sector are decoupled,  $T'$  redshifts due to the expansion of the Universe, as a non-relativistic matter.

In Fig. 3, we show the allowed region in  $m - g_X$  plane from the relic density (scattered points) and thermalisation constraints (green) along with the constraints from the measurement of diffuse  $\gamma$ -ray flux by EGRET (yellow), INTEGRAL (blue).

## 5. $\nu$ and $\gamma$ ray signals from DM annihilation

In this model, it is possible to investigate the prospect of detecting  $\nu$  and  $\gamma$  ray signals from DM annihilation via one step cascade processes such as  $\chi_i \chi_i \rightarrow A (A \rightarrow XY)$ . For the  $\gamma$  rays,  $A$ ,  $X$ , and  $Y$  are  $h_d$ ,  $\gamma$  and  $\gamma$  respectively whereas for the neutrinos in the final state, the intermediate particle, instead of  $h_d$ , is the  $U(1)_X$  gauge boson  $Z'$ .

•  **$\nu$  signal from DM annihilation:** In our model, the kinetic mixing portal can produce neutrino signal from dark matter annihilation. For the exact degenerate case (i.e.  $\delta_m = 0$  where  $\delta_m \equiv (m_{\chi_i} - m_{Z'(h_d)})/m_{\chi_i}$ ), the neutrino spectrum is a line spectrum. Here we have considered the

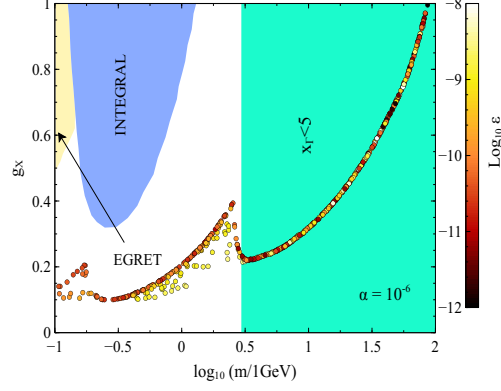


**Figure 3:** Allowed values of  $g_X$  while varying  $m$  between 0.1 GeV to 100 GeV for a fixed value of scalar mixing angle  $\alpha$ . The colour bar indicates the corresponding allowed range of  $\epsilon$ . The light yellow and the light blue regions are disallowed from indirect detection constraints coming from diffuse  $\gamma$  ray background. The Figure is taken from [5].

following cascade process  $\chi_i \chi_i \rightarrow Z' (Z' \rightarrow \bar{\nu}_\mu \nu_\mu)$  to calculate the  $E_\nu^2$  weighted differential  $\nu_\mu$  flux and compared with the available data from Super-Kamiokande collaboration where  $E_\nu$  is the energy of the neutrino. We have checked that the model predicted  $\nu_\mu$  flux is several orders of magnitude smaller than the measured flux by SK collaboration.

•  **$\gamma$  signal from DM annihilation:** In our model,  $\gamma$  ray flux from DM annihilation is composed of three different components such as final state radiation (FSR),  $\gamma$ -ray line signal, and inverse compton scattering (ICS). In Fig. 4, we show the variation of  $E_\gamma^2$  weighted differential photon flux as a function of the energy of the emitted photon ( $E_\gamma$ ) considering  $\delta_m = 0$ . The data points in the figure represent the measured diffuse  $\gamma$ -ray background flux by EGRET [7], INTEGRAL [8], and Fermi-LAT [9].

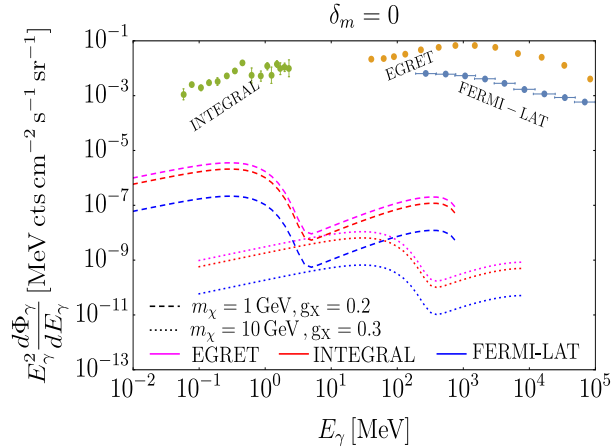


**Figure 4:** Variation of differential  $\gamma$ -ray flux from dark matter annihilation as a function of energy of the emitted photons for two different benchmark points, allowed from relic density constraint. Figure is taken from [5].

## 6. Conclusion

In this work we have studied the evolution of a thermally decoupled multicomponent dark sector in an anomaly free  $U(1)_X$  extension of SM where the dark sector contains two Majorana fermion DM candidate  $\chi_1, \chi_2$ , a dark vector boson  $Z'$ , and the dark Higgs  $h_d$ . Assuming the dark sector particles are degenerate/quasi-degenerate, we have found that the freeze-out of DM occur at much later time in comparison to the WIMP scenario due to the degeneracy of the DS particles. Considering all possible  $2 \rightarrow 2$  and  $3 \rightarrow 2$  processes within the dark sector, we have studied the relic density of DM and temperature evolution of the dark sector. We have investigated indirect detection constraints along with the other constraints from cosmological, astrophysical, and laboratory searches and found that for degenerate dark sector all the constraints can be easily satisfied. However we have shown in [5] that for non-degenerate dark sector, a significant portion of the model parameter space has been excluded by the measurement of cosmic microwave background anisotropy, positron flux by AMS-02, and diffuse  $\gamma$ -ray background flux by INTEGRAL.

## References

- [1] M. Pospelov, A. Ritz and M. B. Voloshin, *Secluded WIMP Dark Matter*, *Phys. Lett. B* **662** (2008) 53 [0711.4866].
- [2] J. L. Feng, H. Tu and H.-B. Yu, *Thermal Relics in Hidden Sectors*, *JCAP* **10** (2008) 043 [0808.2318].
- [3] X. Chu, T. Hambye and M. H. Tytgat, *The Four Basic Ways of Creating Dark Matter Through a Portal*, *JCAP* **05** (2012) 034 [1112.0493].
- [4] T. Hambye, M. H. Tytgat, J. Vandecasteele and L. Vanderheyden, *Dark matter from dark photons: a taxonomy of dark matter production*, *Phys. Rev. D* **100** (2019) 095018 [1908.09864].
- [5] A. Biswas, S. Ganguly and S. Roy, *When freeze-out occurs due to a non-Boltzmann suppression: a study of degenerate dark sector*, *JHEP* **06** (2021) 108 [2011.02499].
- [6] J. A. Dror, E. Kuflik and W. H. Ng, *Codecaying Dark Matter*, *Phys. Rev. Lett.* **117** (2016) 211801 [1607.03110].
- [7] A. W. Strong, I. V. Moskalenko and O. Reimer, *Diffuse galactic continuum gamma rays. A Model compatible with EGRET data and cosmic-ray measurements*, *Astrophys. J.* **613** (2004) 962 [astro-ph/0406254].
- [8] L. Bouchet, A. W. Strong, T. A. Porter, I. V. Moskalenko, E. Jourdain and J.-P. Roques, *Diffuse emission measurement with INTEGRAL/SPI as indirect probe of cosmic-ray electrons and positrons*, *Astrophys. J.* **739** (2011) 29 [1107.0200].
- [9] FERMI-LAT collaboration, *The Spectrum of the Isotropic Diffuse Gamma-Ray Emission Derived From First-Year Fermi Large Area Telescope Data*, *Phys. Rev. Lett.* **104** (2010) 101101 [1002.3603].